Am J Transl Res 2018;10(4):1071-1084
www.ajtr.org /ISSN:1943-8141/AJTR0071304

Original Article

Niclosamide ethanolamine improves diabetes and diabetic kidney disease in mice

Pengxun Han[1*], Mumin Shao[2*], Lan Guo[4], Wenjing Wang[1], Gaofeng Song[1], Xuewen Yu[2], Chunlei Zhang[3], Na Ge[1], Tiegang Yi[1], Shunmin Li[1], Heng Du[4], Huili Sun[1]

[1]Department of Nephrology, [2]Pathology, [3]Clinical Laboratory, Shenzhen Traditional Chinese Medicine Hospital, The Fourth Clinical Medical College of Guangzhou University of Chinese Medicine, Shenzhen 518033, Guangdong, China; [4]Department of Biological Sciences, The University of Texas at Dallas, Richardson, Texas, USA. [*]Equal contributors.

Received December 21, 2017; Accepted March 10, 2018; Epub April 15, 2018; Published April 30, 2018

Abstract: Diabetes and its renal complications are major medical challenges worldwide. There are no effective drugs currently available for treating diabetes and diabetic kidney disease (DKD), especially in type 1 diabetes (T1D). Evidence has suggested that niclosamide ethanolamine salt (NEN) could improve diabetic symptoms in mice of type 2 diabetes (T2D). However, its role in T1D and DKD has not been studied to date. Here we report that NEN could protect against diabetes in streptozotocin (STZ) induced T1D mice. It increased serum insulin levels, corrected the unbalanced ratio of α-cells to β-cells, and induced islet morphologic changes under diabetic conditions. In addition, NEN could impede the progression of DKD in T1D. Specifically, it reduced urinary albumin levels, NAG, NGAL and TGF-β1 excretion, ameliorated renal hypertrophy, alleviated podocyte dysfunction, and suppressed the renal cortical activation of mTOR/4E-BP1 signaling pathway. Moreover, it is hepatoprotective and does not exhibit heart toxicity. Therefore, these findings open up a completely novel therapy for diabetes and DKD.

Keywords: Niclosamide ethanolamine salt, diabetes, diabetic kidney disease

Introduction

The incidence and prevalence of diabetes have increased markedly throughout the world [1, 2]. As one of the most frequent complication of both types of diabetes, diabetic kidney disease (DKD) has become the leading cause of chronic kidney disease [3]. As such, the prevention and control of diabetes and its renal complication has become a major medical challenge [4]. However, no effective drugs are currently available for treating DKD, especially in type 1 diabetes (T1D).

T1D and type 2 diabetes (T2D) are characterized by pancreatic β-cell loss and dysfunction [5]. Although the etiology and pathogenesis underlying these conditions are distinct, they share hyperglycemia, similar clinical symptoms, and common pathological characteristics and complications. Of note, epidemiologic data suggest that diabetes is closely associated with many forms of cancer [6]. Moreover, some medications used to treat hyperglycemia exhibit obvious anticancer effects. As a first line antidiabetic agent, metformin could suppress glioma cell proliferation by inhibiting mTOR/4EBP1 activity [7, 8]. The mTOR/4EBP1 signaling pathway is not only crucial for cancer cell proliferation and growth, but it has also been implicated in diabetes and DKD [9, 10]. Although accumulating evidence has confirmed the effects of various antidiabetic medications on cancer incidence and mortality, but on the other hand, the effects of anticancer therapies on diabetes have rarely been studied [11]. Careful screening for anticancer drugs might improve diabetes is necessary and meaningful.

Niclosamide is an FDA approved antihelmintic drug [12]. Recently, a series of studies demonstrated that niclosamide exhibits antitumor activity in acute myelogenous leukemia [13], colon cancer [14], glioblastoma [15], lung cancer [16], breast cancer [17] and ovarian cancer [18]. In addition, niclosamide could modulate

dendritic cells activation and function [19], inhibit Zika virus replication [20], ameliorate joint inflammation [21], prevent systemic sclerosis [22] and improve sclerodermatous graft-versus-host disease [23]. Moreover, niclosamide is an efficacious mTOR inhibitor which may serve as a potential antidiabetic drug [24, 25]. Niclosamide ethanolamine salt (NEN) is the salt form of niclosamide, it is more water soluble. Interestingly, it improved diabetic symptoms in db/db mice by inducing mild mitochondrial uncoupling [26]. However, its role in T1D and DKD has not been studied.

The present study was performed to determine the role of NEN in T1D and DKD, and investigate the potential mechanisms behind these effects.

Materials and methods

Mice

Animal studies were approved by the Guangzhou University of Chinese Medicine Institutional Animal Care and Use Committee and were performed under protocols in accordance with relevant guidelines and regulations. Eight-week old specific pathogen free male C57BL/6J mice (18-22 g) obtained from Guangdong Medical Laboratory Animal Center were randomly allocated into three groups (n=8-10 per group): the T1D control (T1D-ctrl), STZ, and STZ + NEN groups. STZ (200 mg/kg, Sigma-Aldrich, St. Louis, MO) was dissolved in citrate buffer (pH 4.6) and injected once intraperitoneally. After one week, mice with fasting blood glucose concentration over 16.7 mmol/l were considered as diabetic mice. T1D-ctrl mice were injected intraperitoneally with an equal volume of vehicle. T1D-ctrl and STZ groups were fed with regular diet, and the STZ + NEN group were fed a regular diet supplemented with 10 g/kg NEN. The treatment started 1 week after STZ injection and lasted 8 weeks. NEN was purchased from Hubei ShengTian HengChuang Biotech Co., Ltd (Wuhan, China).

Physiological and metabolic parameters

Fasting blood glucose was measured using blood glucose meter (Roche, Basel, Switzerland). Urine was collected using metabolic cages (Tecniplast, Buguggiate, Italy). At the end of the experiment, mice were sacrificed, then blood samples, pancreas, and kidney tissues were collected. HbA_{1C} levels were measured using an Ultra2 HbA_{1C} Analyzer (Primus, Kansas City, MO). Urine and serum biochemical indices (urine glucose and NAG, serum creatinine, urea, ALT, AST, TP, ALB, CK and LDH) were detected using automatic biochemical analyzer (Roche, Basel, Switzerland).

Tissue preparation

Immediately after the mice were sacrificed, the pancreas and kidneys were dissected, weighed, and rinsed in phosphate buffered saline (PBS). Then, 10% formalin-fixed pancreas and kidney tissues were used for histopathological examination and immunofluorescence staining. The renal cortex (sized 1 mm^3) was fixed in 2.5% glutaraldehyde and then post-fixed in 1% osmic acid for electron microscopy. The remaining renal tissues were immediately snap-frozen in liquid nitrogen and stored at -80°C for later analysis.

Light microscopy

Paraffin-embedded pancreas sections (3 μm) were stained with H&E to measure the mean islet area. Kidney sections (4 μm) were stained with Periodic acid-Schiff (PAS) to evaluate renal morphological changes. In each pancreas section, 4-10 photographs were selected to calculate the mean islet area. A total of 30-50 renal glomerular tuft areas (GTAs), 20-30 renal glomerular mesangial matrix areas, 40-110 proximal renal tubular (PAS staining possessing brush border) areas and tubular lumen areas (axial ratio less than 1.5) were measured using NIS-Elements imaging software Version 4.10 (Nikon, Tokyo, Japan). The renal glomerular tuft volume (GTV) was calculated using the method developed by Weibel as previously described [27]. The tubular wall area was calculated by subtracting the tubular lumen area from the renal tubular area.

Electron microscopy (EM)

Image J software was used to analyze the images collected by EM (JEM-1400, JEOL, Tokyo, Japan). A total of 9-14 photographs in each sample were selected to measure the glomerular basement membrane (GBM) and tubular basement membrane (TBM) thickness using the grid intersect method. In addition, 6-10 photographs in each sample were selected to determine the foot process width (FPW), which

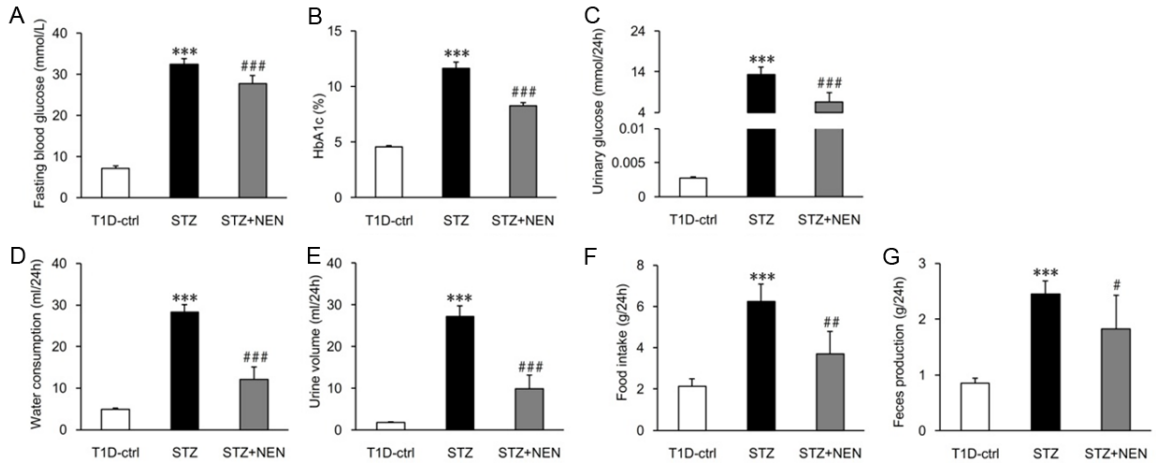

Figure 1. NEN protects against hyperglycemia and improves diabetic symptoms in mice. A-G. In T1D-ctrl, STZ, and STZ + NEN group mice, NEN treatment started when T1D was established (1 week after STZ injection). After 8 weeks of treatment, indicators of glucose metabolism and diabetic symptoms were evaluated. A. Fasting blood glucose. B. Glycated HbA1c. C. Urinary glucose. D. Water consumption. E. Urine volume. F. Food intake. G. Feces production. n=6-8 per group. ***P<0.001 vs. the control group. #P<0.05, ##P<0.01 and ###P<0.001 vs. the STZ group.

is described in nanometers. The average podocyte FPW was calculated using a previously described method [27].

Immunostaining analysis

Briefly, pancreas and kidney slices were deparaffinized and rehydrated. Then, they were subjected to antigen retrieval by boiling in citric acid buffer (pH 6) for 20 min. After rinsing three times with PBS, the pancreas sections were incubated with primary antibodies against insulin (1:400) and glucagon (1:500), and the kidney sections were incubated with primary antibodies against nephrin (1:50) and synaptopodin (1:50) overnight at 4°C. The sections were then washed with rinse buffer, and incubated for 1 hour at room temperature with Alexa Fluor-conjugated secondary antibodies. The resulting images were visualized and captured on a confocal microscope (LSM710, Carl Zeiss, Oberkochen, Germany). A total of 4-10 photographs were randomly selected in each pancreas section to calculate the insulin- and glucagon-positive area. The insulin antibody was from Cell Signaling Technology (Danvers, MA) and the glucagon antibody was from abcam (Cambridge, U.K.). The nephrin and synaptopodin antibodies were from Progen (Heidelburg, Germany).

ELISA

Serum insulin (Merck Millipore, Danvers, MA), serum glucagon (R&D Systems, Minneapolis, MN), urine albumin (Bethyl Laboratories), urine TGF-β1 (R&D Systems, Minneapolis, MN) and NGAL (R&D Systems, Minneapolis, MN) were detected by ELISA according to the manufacturer's instructions.

Immunoblotting analysis

Snap-frozen kidney tissues were homogenized in lysis buffer and prepared in sample loading buffer (Bio-Rad, Hercules, CA). The proteins were separated on SDS-PAGE gels and transferred to polyvinylidene difluoride (PVDF) membranes (Merck Millipore, Danvers, MA). After blocking in TBS buffer containing 5% nonfat dry milk for 1 h at room temperature, the membranes were incubated and gently shaken overnight at 4°C with primary antibodies. After washing with TBS, the membranes were incubated with secondary antibodies for 1 h at room temperature with shaking. After washing, the protein bands were detected and analyzed by a ChemiDoc™ MP Imaging System (Bio-Rad, Hercules, CA). β-actin or α-tubulin were used as the loading control. The results are expressed as the integrated optical density relative to β-actin or α-tubulin. Primary antibodies against p-mTOR (Ser2448) (1:1000), mTOR (1:1000), p-4E-BP1 (Thr37/46) (1:1000), p-4E-BP1 (Thr70) (1:1000), total 4E-BP1 (1:1000), and α-tubulin (1:1000) were from Cell Signaling Technology (Danvers, MA). The nephrin antibody (1:500) was from Progen (Heidelburg, Germany) and the β-actin antibody (1:10000) was from Sigma Aldrich (St. Louis, MO).

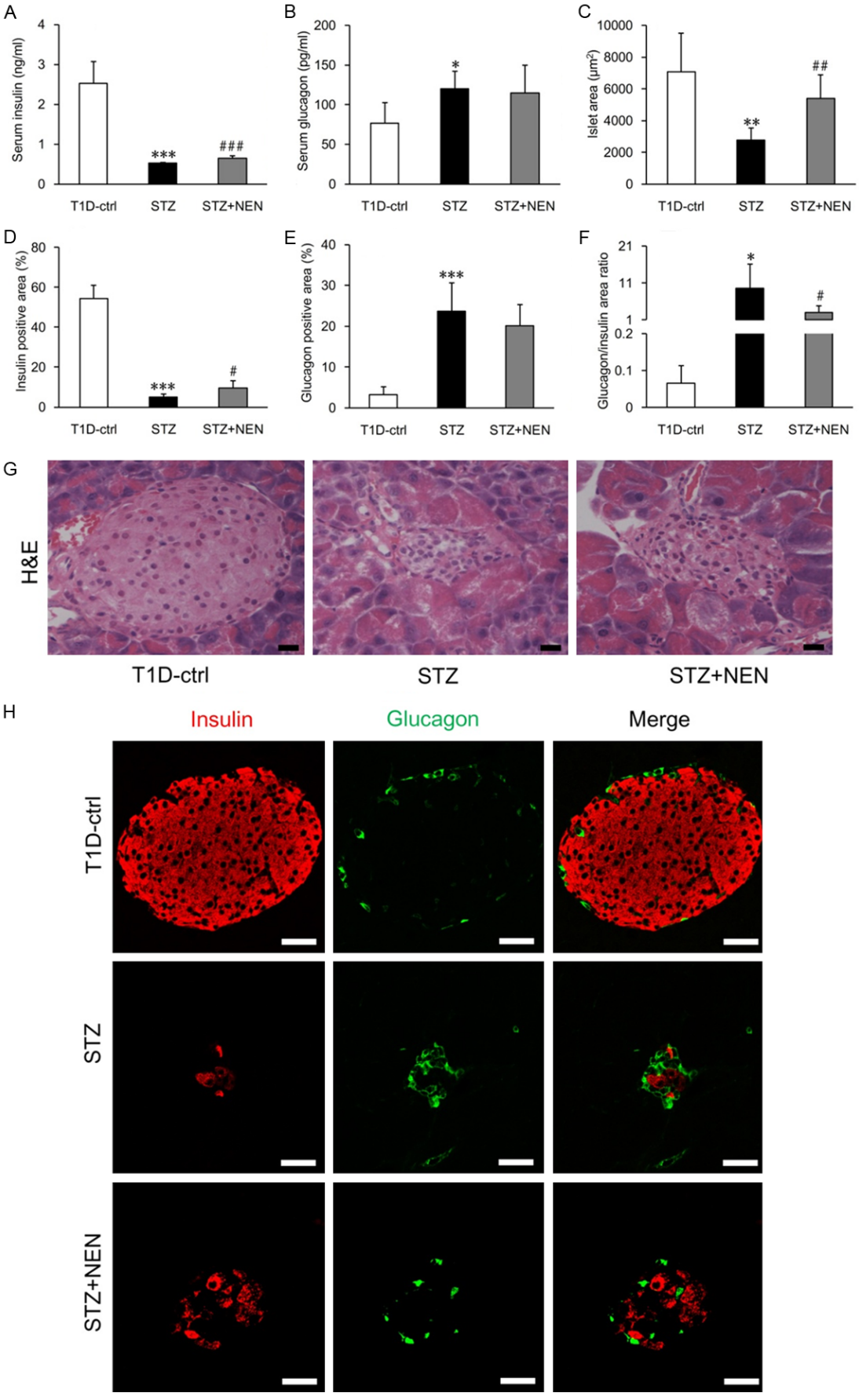
A
Serum insulin (ng/ml)
4
3
2
1
0
***
###
T1D-ctrl
STZ
STZ+NEN
B
Serum glucagon (pg/ml)
200
150
100
50
0
*
T1D-ctrl
STZ
STZ+NEN
C
Islet area (μm²)
10000
8000
6000
4000
2000
0
**
##
T1D-ctrl
STZ
STZ+NEN
D
Insulin positive area (%)
80
60
40
20
0
***
#
T1D-ctrl
STZ
STZ+NEN
E
Glucagon positive area (%)
40
30
20
10
0
***
T1D-ctrl
STZ
STZ+NEN
F
Glucagon/insulin area ratio
21
11
1
0.2
0.1
0
*
#
T1D-ctrl
STZ
STZ+NEN
G
H&E
T1D-ctrl
STZ
STZ+NEN
H
Insulin
Glucagon
Merge
T1D-ctrl
STZ
STZ+NEN

Figure 2. NEN improves pancreatic islet function. (A) Serum insulin (n=6-8 per group) and (B) serum glucagon (n=5 per group) levels were assessed in T1D diabetic model at the end of the study. (G) Pancreatic H&E staining was performed to measure the mean islet area. Scale bars, 25 μm. (C) Bar graphs denote the quantification and statistical analysis of the mean islet area in different groups (n=4-8 per group). (H) Insulin (red) and glucagon (green) coimmunostaining was performed on pancreatic sections to assess the percentage of insulin- and glucagon-positive area per islet. Scale bars, 25 μm. (D-F) The quantification and statistical analysis of the insulin-positive area, glucagon-positive area, and glucagon: insulin area ratio in different groups (n=4-6 per group). **P*<0.05, ***P*<0.01, and ****P*<0.001 vs. the control group. #*P*<0.05, ##*P*<0.01 and ###*P*<0.001 vs. the STZ group.

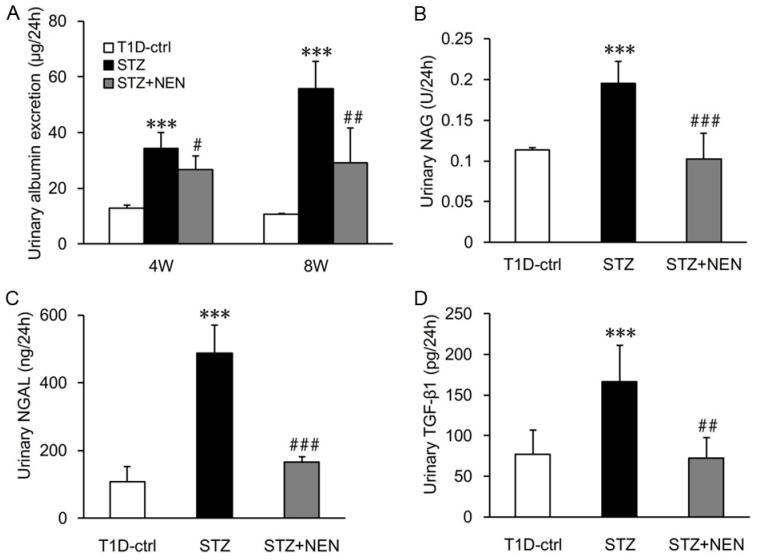

Figure 3. NEN reduces urinary albumin, NAG, NGAL and TGF-β1 excretion. A. Urinary albumin excretion (μg/24 h) in different groups of mice at 4 weeks and 8 weeks after the onset of T1D. B-D. Urinary NAG, NGAL and TGF-β1 excretion at 8 weeks in the T1D model. n=6-8 per group. ****P*<0.001 vs. the control group. #*P*<0.05, ##*P*<0.01 and ###*P*<0.001 vs. the STZ group.

Statistical analysis

Data are expressed as mean ± SD. Statistical differences between two groups were analyzed using unpaired Student's *t* tests. Differences among multiple groups were analyzed using one-way ANOVA. Statistical analyses were performed using SPSS statistical software, version 16.0, and *P*<0.05 was considered statistically significant.

Results

NEN protects against hyperglycemia and improves diabetic symptoms in T1D

We first investigated the effects of NEN on blood glucose and metabolic symptoms that are recognized as the diagnostic criteria for diabetes. Compared with control mice, T1D STZ mice exhibited higher fasting blood glucose, glycated HbA1c, and urinary glucose levels at 8 weeks. NEN significantly reduced these indices in T1D after 8 weeks treatment (**Figure 1A**, **1C**). STZ group mice displayed typical diabetic symptoms including polydypsia, polyuria, polyphagia, and increased feces production at 8 weeks. NEN obviously improved these metabolic symptoms (**Figure 1D-G**).

NEN increases serum insulin, corrects the unbalanced ratio of α to β-cells, and induces islet morphologic changes under diabetic conditions

Pancreatic islet dysfunction plays a critical role in diabetes progression. Therefore, we explored the impact of NEN on the pancreas. At 8 weeks, mice in STZ group exhibited decreased serum insulin and increased glucagon levels (**Figure 2A**, **2B**). Hematoxylin and eosin (H&E) staining showed the mean islet area was reduced significantly (**Figure 2C**, **2G**). Insulin (red) and glucagon (green) coimmunostaining revealed that the insulin-positive area in the islets was decreased, the glucagon-positive area was increased, and the glucagon/insulin area ratio was increased obviously (**Figure 2D-F**, **2H**). NEN treatment raised serum insulin levels and the insulin-positive area (**Figure 2A**, **2D**). Although NEN did not significantly influence serum glucagon levels and the glucagon-positive area in islets (**Figure 2B**, **2E**), it significantly increased the mean islet area and restored the glucagon: insulin area ratio (**Figure 2C**, **2F**).

NEN reduces urinary albumin, NAG, NGAL, and TGF-β1 excretion

Albuminuria is an early clinical manifestation of DKD and reflects glomerulopathy. Therefore, we next measured urinary albumin excretion to verify the renal protective effects of NEN in

Table 1. Changes in serum biochemical indices in various groups

	T1D-ctrl	STZ	STZ + NEN
Creatinine (μmol/L)	13.2±4.4	15.3±4.6	14.4±4.6
Urea (mmol/L)	13.3±1.6	16.9±3.4**	13.2±2.0#
ALT (U/L)	38.2±11.5	60.4±19.6**	40.1±7.5##
AST (U/L)	152.8±74.0	178.2±60.5	140.1±33.1
TP (g/L)	60.7±2.1	50.0±2.4***	54.4±2.9##
ALB (g/L)	40.1±1.7	33.1±2.6***	37.7±2.9##
CK (U/L)	1606.1±569.2	1762.8±675.3	1406.4±496.0
LDH (U/L)	692.3±144.2	622.4±168.9	515.2±79.5

Data are shown as mean ± SD, n=6-8 per group, $^{**}P<0.01$ and $^{***}P<0.001$ vs. the T1D-ctrl group. $^{\#}P<0.05$ and $^{\#\#}P<0.01$ vs. the STZ group.

DKD. Compared with control mice, urinary albumin excretion was increased significantly in STZ group mice, and reduced significantly by NEN treatment (**Figure 3A**). Urinary NAG (N-acetyl-β-d-glucosamine-dase), NGAL (neutrophil gelatinase-associated lipocalin) and TGF-β1 excretion were also increased remarkably at 8 weeks in STZ mice. NEN treatment significantly reduced these urinary biomarkers (**Figure 3B-D**). In addition, as shown in **Table 1**, serum creatinine and urea levels indicated that NEN did not significantly affect renal function in diabetic model.

NEN decreases enlarged diabetic kidney and ameliorates glomerular and tubular hypertrophy

Renal hypertrophy is the main pathological characteristic of early diabetes. Therefore, we examined the impact of NEN on renal pathologic alterations. As shown in **Figure 4A**, the body weight of mice in the STZ group was reduced significantly at 8 weeks. Out of proportion to the altered body weight, the kidney weight was similar to that of mice in the control group (**Figure 4B**). However, the kidney: body weight ratio in STZ mice increased obviously and NEN treatment reduced it significantly (**Figure 4C**).

As shown in **Figure 4D**, **4E**, mice in STZ group mice displayed larger GTA and bigger GTV, and NEN treatment reversed these changes to a nearly normal state. Although there was no significant difference in these tubular alterations between the STZ and control group (**Figure 4F-H**). NEN therapy significantly reduced the size of the proximal tubule (**Figure 4F-H**). A previous study demonstrated that the glomeruli comprise a small proportion of the kidney and that tubule growth is the largest contributor to renal hypertrophy [28]. The current results also revealed that the renal tubular alterations were consistent with the variation of kidney weight when considering the body weight. Images of the kidneys and PAS staining showed these characteristics in each group (**Figure 4I-K**).

NEN reduces glomerular mesangial expansion and attenuates GBM thickening

Glomerular hypertrophy is characterized by mesangial expansion and GBM thickening. So we measured the mesangial matrix fraction and GBM thickness to further confirm the effects of NEN on glomerular size. At the end of the study, PAS staining revealed that mesangial matrix fraction increased significantly in STZ mice (**Figure 5A**, **5D**). Electron microscopy (EM) photographs (**Figure 5B**) also revealed that significant mesangial matrix accumulation and expansion. NEN treatment diminished the mesangial expansion significantly (**Figure 5A**, **5B**, **5D**). As shown in **Figure 5C**, **5E**, the GBM thickened significantly in STZ mice and NEN attenuated these changes.

NEN alleviates podocyte dysfunction

Podocyte injury is a key determinant of albuminuria and a critical factor in DKD progression. The ability of NEN to reduce albuminuria suggested that it might exert protective effects on podocytes. To further elucidate the impacts of NEN on podocyte dysfunction, we measured podocyte FPW and explored nephrin alteration in kidney. The FPW was wider in STZ mice compared with control group mice (**Figure 6A**, **6B**), and the slit diaphragm seemed to aggregate and distort (**Figure 6B**). NEN treatment reduced the size of the FPW and improved the slit diaphragm morphological alterations (**Figure 6A**, **6B**).

Nephrin is the first identified slit diaphragm component that plays a key role in podocyte dysfunction [29]. In the T1D diabetic model, immunoblotting revealed that the nephrin content in renal cortical homogenates was increased significantly (**Figure 6C**, **6D**). Under normal conditions, nephrin colocalized appro-

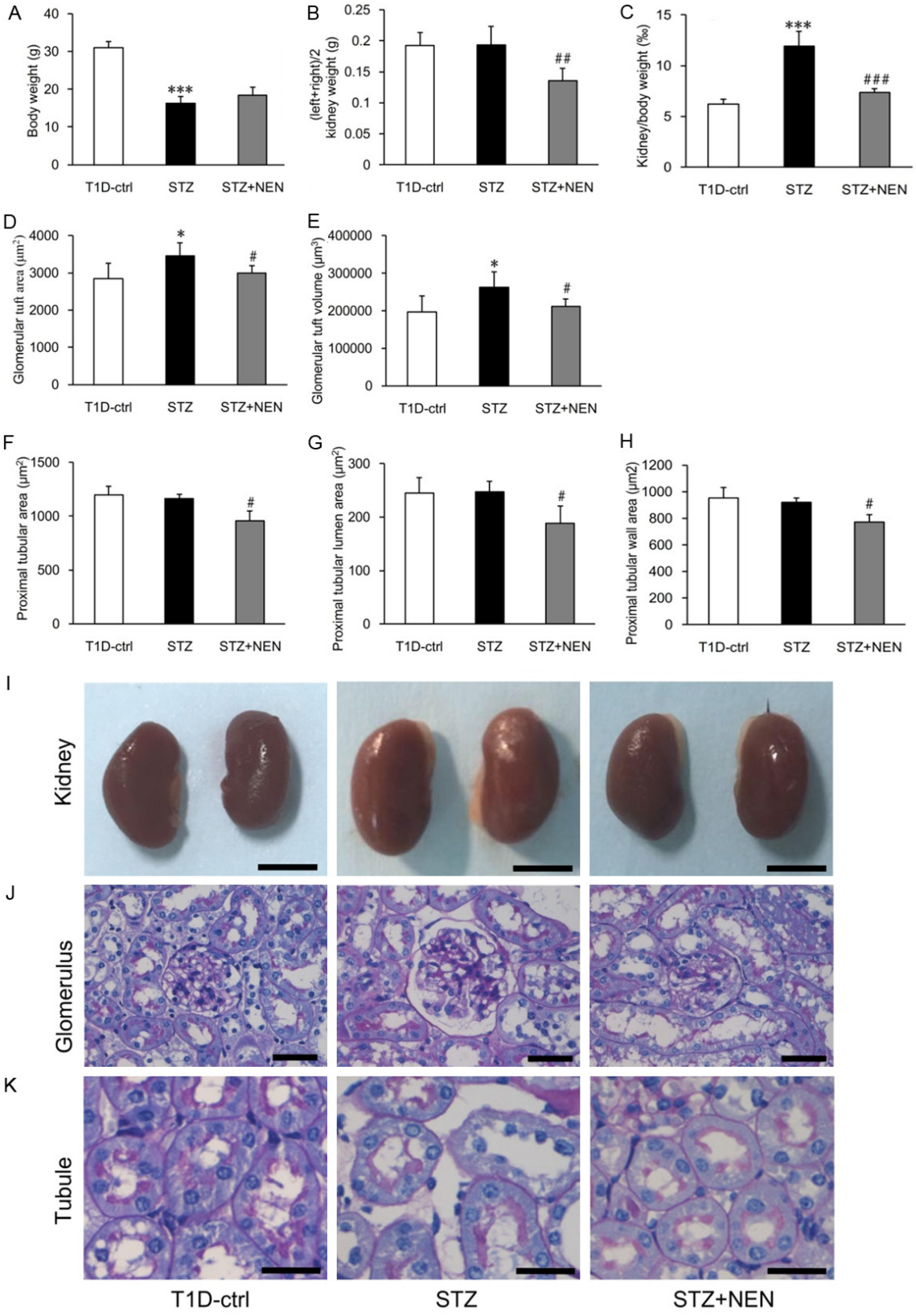

Figure 4. Effects of NEN on body weight, diabetic kidney weight, and glomerular and proximal tubule size. (A) Body weight, (B) kidney weight, and (C) kidney: body weight ratio in each group mice at the end of the study. (I) Representative kidney images. Scale bars, 0.5 cm. (D, E) Bar graphs indicating the GTA and GTV of each group in the

T1D diabetic model. (J) PAS staining for the glomerulus. Scale bars, 50 μm. (F-H) Bar graphs indicating the proximal tubular area, lumen, and wall area in each group. (K) PAS staining for the renal tubules. Scale bars, 25 μm. n=6-8 per group. *P<0.05 and ***P<0.001 vs. the control group. #P<0.05, ##P<0.01, and ###P<0.001 vs. the STZ group.

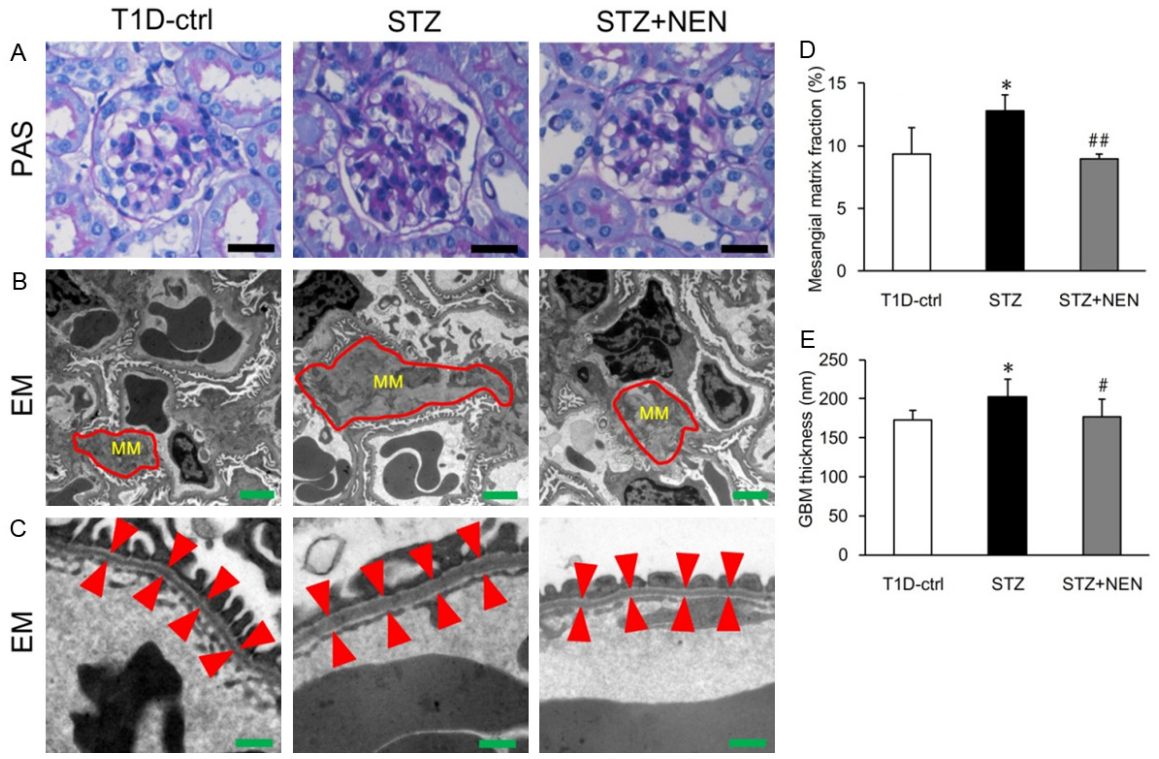

Figure 5. NEN diminishes glomerular mesangial expansion and attenuates GBM thickening. A. Kidney sections stained with PAS to measure the mesangial matrix fraction at the end of the experiment. Scale bars, 25 μm. D. Bar graphs representing the quantification and statistical analysis of the data. n=4 per group. B. Typical EM photographs showing obvious mesangial matrix accumulation and expansion. MM, mesangial matrix. Scale bars, 2 μm. C. Representative EM images of the GBM. The arrowheads indicate the thickness of the GBM. Scale bars, 500 nm. E. Bar graphs showing the quantification and statistical analysis of the data. n=5-8 per group. *P<0.05 vs. the control group. #P<0.05 and ##P<0.01 vs. the STZ group.

priately with synaptopodin along the membrane of the podocytes. However, under diabetic conditions, it failed to colocalize well with synaptopodin (**Figure 6E**). The confocal microscopic analysis of the renal glomeruli indicated that nephrin was scattered, with granular aggregation and cytoplasm localization in STZ group (**Figure 6F**). NEN treatment reduced the nephrin content and restored these abnormal pathological alterations to a nearly normal state (**Figure 6C-F**).

NEN attenuates the thickened proximal renal TBM

The TBM thickening of nonatrophic tubules is apparent in early diabetes and it becomes more conspicuous as diabetes progresses. At the end of the experiment, the TBM was thicker in STZ group mice and NEN made it thinner significantly (**Figure 7A**, **7B**). The microvilli shown in **Figure 7A** indicated hat the TBM was located on proximal renal tubules.

NEN suppresses the renal cortical activation of mTOR/4E-BP1

The mTOR/4EBP1 signaling pathway is implicated in diabetes and DKD progression. Compared with control mice, mice in STZ group expressed higher renal cortical levels of p-mTOR (Ser2448), p-4E-BP1 (Thr37/46), p-4E-BP1 (Thr70), and total 4E-BP1, as determined by western blotting. NEN treatment suppressed the activation of these proteins (**Figure 8**). TGF-β1 promotes renal cell hypertrophy and

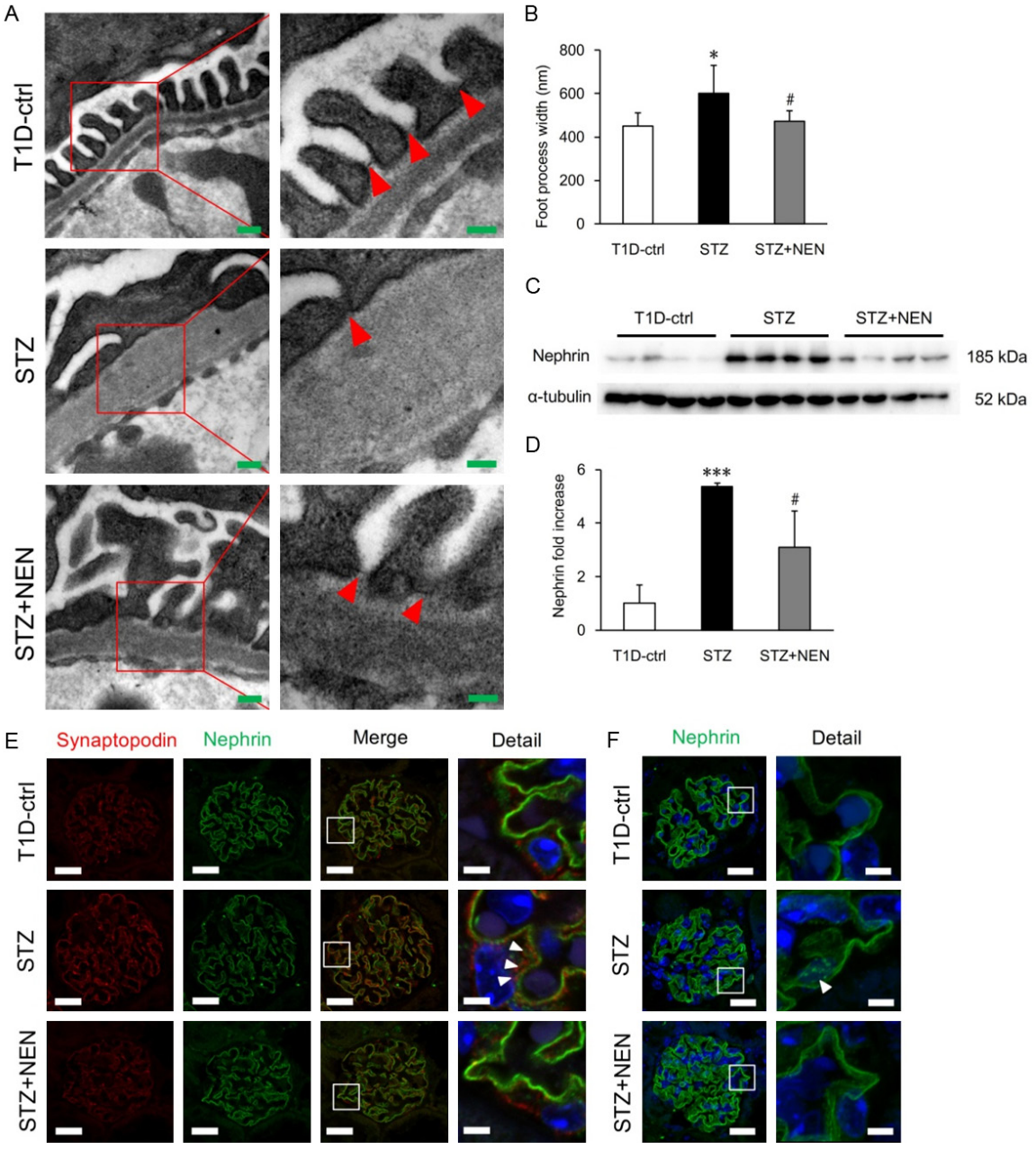

Figure 6. NEN alleviates podocyte dysfunction. A. Glomerular podocyte EM images were used to measure the FPW. The arrowheads indicate slit diaphragm morphological alterations. Scale bars, 200 nm (left) and 100 nm (right). B. Bar graphs showing the FPW results. n=6-8 per group. C. Western blot images showing nephrin expression in renal cortical homogenates. Original full-size blots are presented in supplementary Figure S1. D. Bar graphs showing the fold-increase in nephrin expression normalized to the internal control α-tubulin. n=4 per group. E. Synaptopodin (red) and nephrin (green) coimmunostaining in kidney sections was performed to determine the localization of nephrin. The arrowheads demonstrate that nephrin failed to colocalize well with synaptopodin. Blue, DAPI staining of the nucleus. Scale bars: from left to right, 15 μm, 15 μm, 15 μm, 5 μm. F. Representative confocal immunofluorescence images of nephrin staining. The arrowheads show that nephrin in the renal glomeruli exhibited scattered granular aggregation and localization to the cytoplasm in STZ group. Blue, DAPI staining of the nucleus. Scale bars: left, 15 μm; right, 5 μm. **P*<0.05 and ****P*<0.001 vs. the control group. #*P*<0.05 vs. the STZ group.

the accumulation of extracellular matrix components. The mTOR/4E-BP1 signaling pathway can also be activated by TGF-β and induce cell growth. The ability of NEN to lower urinary TGF-

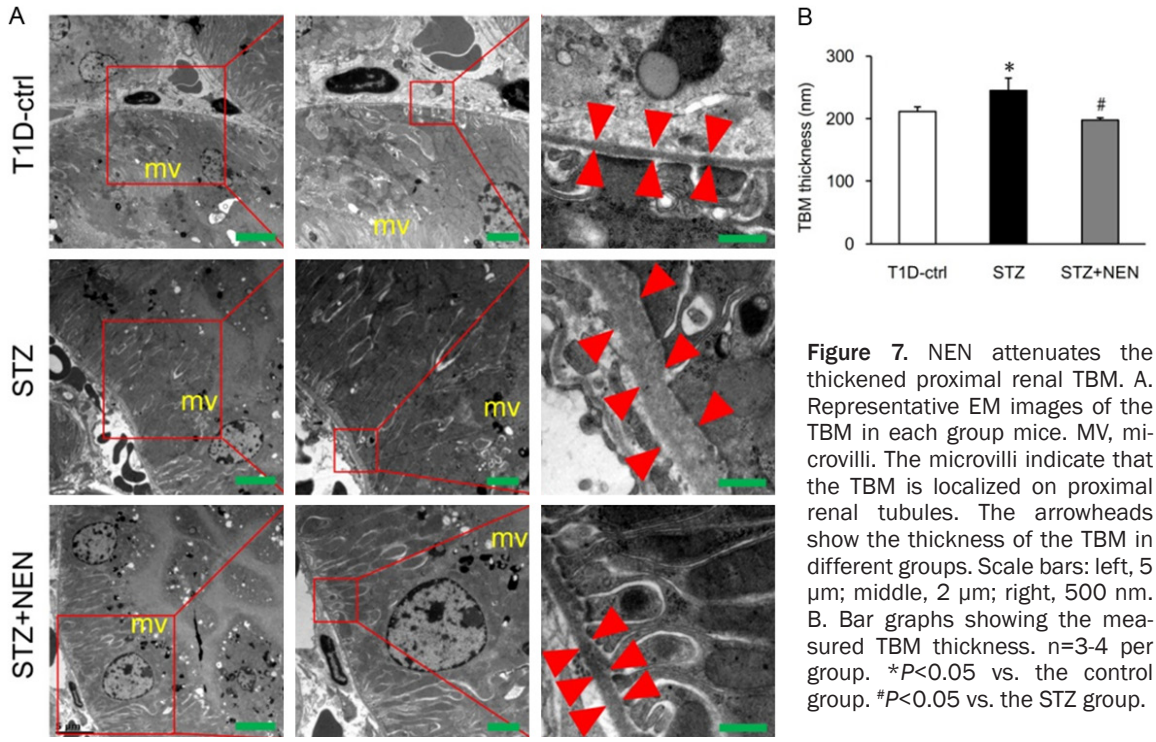

Figure 7. NEN attenuates the thickened proximal renal TBM. A. Representative EM images of the TBM in each group mice. MV, microvilli. The microvilli indicate that the TBM is localized on proximal renal tubules. The arrowheads show the thickness of the TBM in different groups. Scale bars: left, 5 μm; middle, 2 μm; right, 500 nm. B. Bar graphs showing the measured TBM thickness. n=3-4 per group. $^{*}P<0.05$ vs. the control group. $^{\#}P<0.05$ vs. the STZ group.

β1 levels well explained its inhibitory effect on renal mTOR/4EBP1 pathway, and these results further support a renal protective role for NEN.

NEN is hepatoprotective and does not exhibit heart toxicity

As shown in **Table 1**, serum CK and LDH levels indicate that NEN does not exhibit cardiac toxicity. Moreover, biochemical indices of hepatic function demonstrated that NEN exerts hepatoprotective effects, and especially targeting to ALT in the diabetic model.

Discussion

Here, we report a novel role for NEN in protecting against diabetes and DKD in STZ induced mouse model of T1D. In this study, NEN treatment reversed hyperglycemia and improved diabetic symptoms in the diabetic model.

Pancreatic β cell loss and dysfunction are central to diabetes. Therefore, we assessed serum insulin levels, measured the islet size, and evaluated the insulin area in pancreatic islets. In STZ-induced T1D mice, NEN treatment for 8 weeks significantly increased serum insulin levels, islet size, and the islet insulin area. These changes could explain the hypoglycemic effects of NEN in T1D.

An increasing amount of data have indicated that islet α-cells and glucagon play critical role in diabetes, and hyperglucagonemia is present in all types of diabetes [30-33]. Consistent with previous studies, serum glucagon levels were increased significantly in the current study. The glucagon area in islets also expanded significantly. The current findings also revealed that the α-cell to β-cell mass ratio in islets was increased significantly in STZ group mice. NEN restored the imbalanced α-cells to β-cell ratio, without obviously altering serum glucagon levels and the glucagon area in islets. This suggests that the protective effects of NEN on diabetes occur largely by improving β-cell function or inducing an α-to-β-like cell conversion.

The current results also demonstrated that NEN could impede the progression of DKD. Early DKD is characterized by albuminuria, increased excretion of urinary NAG, NGAL and TGF-β1, mesangial expansion, glomerular and renal tubular hypertrophy, and GBM and TBM thickening. NEN administration significantly reduced albuminuria, decreased urinary excretion of NAG, NGAL, and TGF-β1, and attenuated

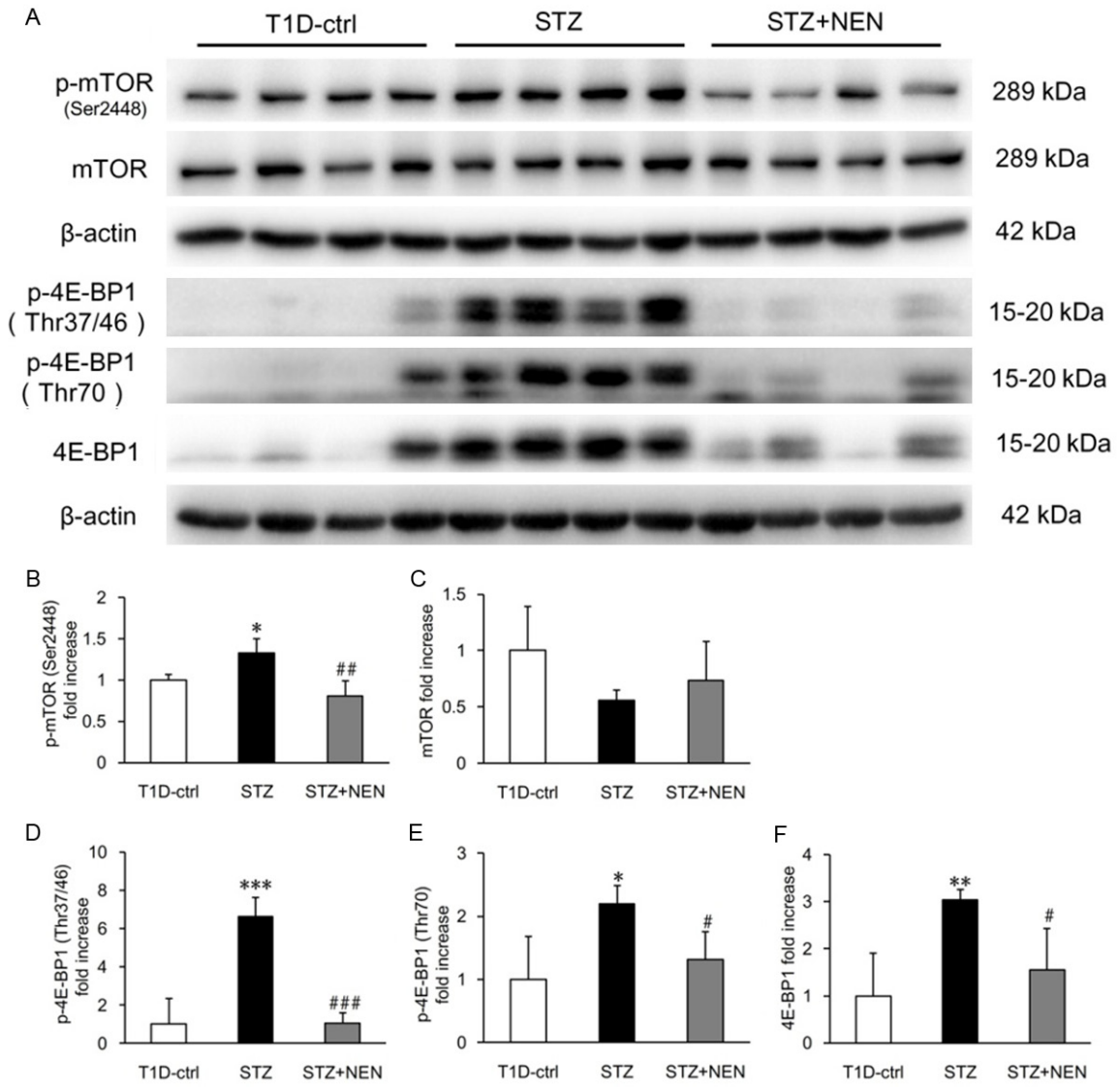

Figure 8. NEN inhibits mTOR/4E-BP1 signaling in the renal cortex. A. Western blot images of p-mTOR (Ser2448), mTOR, p-4E-BP1 (Thr37/46), p-4E-BP1 (Thr70), and total 4E-BP1 in the renal cortex of mice in each group. Original full-size blots are presented in Figure S2. B-F. Bar graphs showing the fold-increase in protein expression after normalization to the internal control β-actin. n=4 per group. **P*<0.05, ***P*<0.01 and ****P*<0.001 vs. the control group. #*P*<0.05 and ##*P*<0.01 vs. the STZ group.

glomerular and tubular injury. As a transmembrane podocyte protein, nephrin plays a crucial role in the interpodocyte slit membrane structure and renal filtration barrier [34]. In T1D STZ rats and nonobese diabetic mice, nephrin-specific mRNA levels increase obviously at an early stage [35]. In diabetic db/db mice, nephrin protein in kidney cortex increased significantly detected by immunoblotting [36]. Consistent with these previous studies, the current immunoblotting results revealed that nephrin levels were increased significantly in the renal cortex. Under normal conditions, most nephrin colocalized well with synaptopodin which is abundant in the vicinity of podocyte membranes. However, under diabetic conditions, confocal microscopy indicated that nephrin exhibited scattered aggregation and was mislocated to the cytoplasm in glomeruli. NEN treatment reduced the nephrin content and improved the pathological alterations to a near normal state. In contrast, other studies reported that glomerular nephrin expression is reduced significantly in diabetes [37, 38]. These contradictory results

may due to a variety of underlying causes, such as diversity in species, duration of diabetes, and different detection methods.

Another major finding in this study is that NEN suppressed the abnormal activation of the mTOR/4E-BP1 signaling pathway in the renal cortex. The mTOR/4E-BP1 signal pathway can be activated by TGF-β and contributes to matrix protein production and cell growth [39]. In the current study, NEN significantly reduced urinary TGF-β excretion which could explain its ability to inhibit mTOR/4E-BP1. The genetic deletion of the mTOR complex in mouse podocytes induced proteinuria and progressive glomerulosclerosis. In contrast, the excessive activation of mTOR is accompanied by DKD, and inhibiting mTOR can protect podocytes and prevent progressive DKD [40, 41]. A previous study demonstrated that treating podocytes with rapamycin significantly downregulated nephrin [42]. This suggests that NEN could lower nephrin levels by inhibiting mTOR. However, the explicit mechanism still needs further investigation.

In addition, NEN does not exhibit heart toxicity and is hepatoprotective. Therefore, it might be a promising antidiabetic drug without potential side effects. It is worth considering whether the renal protective effects of NEN depend on its hypoglycemic effects. A recent study revealed that phosphate niclosamide (the water-soluble form of niclosamide) significantly reduced proteinuria, glomerulosclrotic lesions, and interstitial fibrosis in a murine model of adriamycin nephropathy. In addition, it ameliorated established renal interstitial fibrosis a murine model of unilateral ureteral obstruction [43]. These studies suggest that NEN exerts direct renal protective effects, but these observations need further validation. Taken together, these findings introduce a completely novel therapy for diabetes and DKD.

Acknowledgements

This study was supported by grants from National Natural Science Foundation of China (81202818, 81673794, 81373565), and Shenzhen Science and Technology Project (JCYJ-20160330171116798, JCYJ20150401163247228).

Disclosure of conflict of interest

None.

Address correspondence to: Huili Sun, Department of Nephrology, Shenzhen Traditional Chinese Medicine Hospital, The Fourth Clinical Medical College of Guangzhou University of Chinese Medicine, 1 Fuhua Road, Futian District, Shenzhen 518033, Guangdong, China. Tel: 86-755-83214509; Fax: 86-755-88356033; E-mail: sunhuili2011@126.com; Heng Du, Department of Biological Sciences, The University of Texas at Dallas, Richardson, Texas, USA. E-mail: heng.du@utdallas.edu

References

[1] Xu Y, Wang L, He J, Bi Y, Li M, Wang T, Jiang Y, Dai M, Lu J, Xu M, Li Y, Hu N, Li J, Mi S, Chen CS, Li G, Mu Y, Zhao J, Kong L, Chen J, Lai S, Wang W, Zhao W and Ning G. Prevalence and control of diabetes in Chinese adults. JAMA 2013; 310: 948-959.

[2] Menke A, Casagrande S, Geiss L and Cowie CC. Prevalence of and trends in diabetes among adults in the united states, 1988-2012. JAMA 2015; 314: 1021-1029.

[3] Zhang L, Long J, Jiang W, Shi Y, He X, Zhou Z, Li Y, Yeung RO, Wang J, Matsushita K, Coresh J, Zhao MH and Wang H. Trends in chronic kidney disease in China. N Engl J Med 2016; 375: 905-906.

[4] Molitch ME, Adler AI, Flyvbjerg A, Nelson RG, So WY, Wanner C, Kasiske BL, Wheeler DC, de Zeeuw D and Mogensen CE. Diabetic kidney disease: a clinical update from kidney disease: improving global outcomes. Kidney Int 2015; 87: 20-30.

[5] Wang P, Fiaschi-Taesch NM, Vasavada RC, Scott DK, Garcia-Ocana A and Stewart AF. Diabetes mellitus--advances and challenges in human beta-cell proliferation. Nat Rev Endocrinol 2015; 11: 201-212.

[6] Garcia-Jimenez C, Gutierrez-Salmeron M, Chocarro-Calvo A, Garcia-Martinez JM, Castano A and De la Vieja A. From obesity to diabetes and cancer: epidemiological links and role of therapies. Br J Cancer 2016; 114: 716-722.

[7] Pernicova I and Korbonits M. Metformin--mode of action and clinical implications for diabetes and cancer. Nat Rev Endocrinol 2014; 10: 143-156.

[8] Liu X, Chhipa RR, Pooya S, Wortman M, Yachyshin S, Chow LM, Kumar A, Zhou X, Sun Y, Quinn B, McPherson C, Warnick RE, Kendler A, Giri S, Poels J, Norga K, Viollet B, Grabowski GA and Dasgupta B. Discrete mechanisms of mTOR and cell cycle regulation by AMPK agonists independent of AMPK. Proc Natl Acad Sci U S A 2014; 111: E435-444.

[9] Laplante M and Sabatini DM. mTOR signaling in growth control and disease. Cell 2012; 149: 274-293.

[10] Reidy K, Kang HM, Hostetter T and Susztak K. Molecular mechanisms of diabetic kidney disease. J Clin Invest 2014; 124: 2333-2340.
[11] Shlomai G, Neel B, LeRoith D and Gallagher EJ. Type 2 diabetes mellitus and cancer: the role of pharmacotherapy. J Clin Oncol 2016; 34: 4261-4269.
[12] Chen W, Mook RA Jr, Premont RT and Wang J. Niclosamide: beyond an antihelminthic drug. Cell Signal 2018; 41: 89-96.
[13] Jin Y, Lu Z, Ding K, Li J, Du X, Chen C, Sun X, Wu Y, Zhou J and Pan J. Antineoplastic mechanisms of niclosamide in acute myelogenous leukemia stem cells: inactivation of the NF-kappaB pathway and generation of reactive oxygen species. Cancer Res 2010; 70: 2516-2527.
[14] Sack U, Walther W, Scudiero D, Selby M, Kobelt D, Lemm M, Fichtner I, Schlag PM, Shoemaker RH and Stein U. Novel effect of antihelminthic Niclosamide on S100A4-mediated metastatic progression in colon cancer. J Natl Cancer Inst 2011; 103: 1018-1036.
[15] Wieland A, Trageser D, Gogolok S, Reinartz R, Hofer H, Keller M, Leinhaas A, Schelle R, Normann S, Klaas L, Waha A, Koch P, Fimmers R, Pietsch T, Yachnis AT, Pincus DW, Steindler DA, Brustle O, Simon M, Glas M and Scheffler B. Anticancer effects of niclosamide in human glioblastoma. Clin Cancer Res 2013; 19: 4124-4136.
[16] You S, Li R, Park D, Xie M, Sica GL, Cao Y, Xiao ZQ and Deng X. Disruption of STAT3 by niclosamide reverses radioresistance of human lung cancer. Mol Cancer Ther 2014; 13: 606-616.
[17] Londono-Joshi AI, Arend RC, Aristizabal L, Lu W, Samant RS, Metge BJ, Hidalgo B, Grizzle WE, Conner M, Forero-Torres A, Lobuglio AF, Li Y and Buchsbaum DJ. Effect of niclosamide on basal-like breast cancers. Mol Cancer Ther 2014; 13: 800-811.
[18] Deng Y, Wang Z, Zhang F, Qiao M, Yan Z, Wei Q, Wang J, Liu H, Fan J, Zou Y, Liao J, Hu X, Chen L, Yu X, Haydon RC, Luu HH, Qi H, He TC and Zhang J. A blockade of IGF signaling sensitizes human ovarian cancer cells to the anthelmintic niclosamide-induced anti-proliferative and anticancer activities. Cell Physiol Biochem 2016; 39: 871-888.
[19] Wu CS, Li YR, Chen JJ, Chen YC, Chu CL, Pan IH, Wu YS and Lin CC. Antihelminthic niclosamide modulates dendritic cells activation and function. Cell Immunol 2014; 288: 15-23.
[20] Xu M, Lee EM, Wen Z, Cheng Y, Huang WK, Qian X, Tcw J, Kouznetsova J, Ogden SC, Hammack C, Jacob F, Nguyen HN, Itkin M, Hanna C, Shinn P, Allen C, Michael SG, Simeonov A, Huang W, Christian KM, Goate A, Brennand KJ, Huang R, Xia M, Ming GL, Zheng W, Song H and Tang H. Identification of small-molecule inhibitors of Zika virus infection and induced neural cell death via a drug repurposing screen. Nat Med 2016; 22: 1101-1107.
[21] Liang L, Huang M, Xiao Y, Zen S, Lao M, Zou Y, Shi M, Yang X and Xu H. Inhibitory effects of niclosamide on inflammation and migration of fibroblast-like synoviocytes from patients with rheumatoid arthritis. Inflamm Res 2015; 64: 225-233.
[22] Morin F, Kavian N, Nicco C, Cerles O, Chereau C and Batteux F. Niclosamide prevents systemic sclerosis in a reactive oxygen species-induced mouse model. J Immunol 2016; 197: 3018-3028.
[23] Morin F, Kavian N, Nicco C, Cerles O, Chereau C and Batteux F. Improvement of sclerodermatous graft-versus-host disease in mice by niclosamide. J Invest Dermatol 2016; 136: 2158-2167.
[24] Fonseca BD, Diering GH, Bidinosti MA, Dalal K, Alain T, Balgi AD, Forestieri R, Nodwell M, Rajadurai CV, Gunaratnam C, Tee AR, Duong F, Andersen RJ, Orlowski J, Numata M, Sonenberg N and Roberge M. Structure-activity analysis of niclosamide reveals potential role for cytoplasmic pH in control of mammalian target of rapamycin complex 1 (mTORC1) signaling. J Biol Chem 2012; 287: 17530-17545.
[25] Li M, Khambu B, Zhang H, Kang JH, Chen X, Chen D, Vollmer L, Liu PQ, Vogt A and Yin XM. Suppression of lysosome function induces autophagy via a feedback down-regulation of MTOR complex 1 (MTORC1) activity. J Biol Chem 2013; 288: 35769-35780.
[26] Tao H, Zhang Y, Zeng X, Shulman GI and Jin S. Niclosamide ethanolamine-induced mild mitochondrial uncoupling improves diabetic symptoms in mice. Nat Med 2014; 20: 1263-1269.
[27] Sun H, Wang W, Han P, Shao M, Song G, Du H, Yi T and Li S. Astragaloside IV ameliorates renal injury in db/db mice. Sci Rep 2016; 6: 32545.
[28] Seyer-Hansen K, Hansen J and Gundersen HJ. Renal hypertrophy in experimental diabetes. A morphometric study. Diabetologia 1980; 18: 501-505.
[29] Kestila M, Lenkkeri U, Mannikko M, Lamerdin J, McCready P, Putaala H, Ruotsalainen V, Morita T, Nissinen M, Herva R, Kashtan CE, Peltonen L, Holmberg C, Olsen A and Tryggvason K. Positionally cloned gene for a novel glomerular protein--nephrin--is mutated in congenital nephrotic syndrome. Mol Cell 1998; 1: 575-582.
[30] Takeda Y, Fujita Y, Honjo J, Yanagimachi T, Sakagami H, Takiyama Y, Makino Y, Abiko A, Kief-

fer TJ and Haneda M. Reduction of both beta cell death and alpha cell proliferation by dipeptidyl peptidase-4 inhibition in a streptozotocin-induced model of diabetes in mice. Diabetologia 2012; 55: 404-412.
[31] Lee Y, Berglund ED, Yu X, Wang MY, Evans MR, Scherer PE, Holland WL, Charron MJ, Roth MG and Unger RH. Hyperglycemia in rodent models of type 2 diabetes requires insulin-resistant alpha cells. Proc Natl Acad Sci U S A 2014; 111: 13217-13222.
[32] Lee YH, Wang MY, Yu XX and Unger RH. Glucagon is the key factor in the development of diabetes. Diabetologia 2016; 59: 1372-1375.
[33] Wang Y, Han C, Zhu W, Wu Z, Liu Y and Chen L. An optical method to evaluate both mass and functional competence of pancreatic alpha- and beta-cells. J Cell Sci 2016; 129: 2462-2471.
[34] Ruotsalainen V, Ljungberg P, Wartiovaara J, Lenkkeri U, Kestila M, Jalanko H, Holmberg C and Tryggvason K. Nephrin is specifically located at the slit diaphragm of glomerular podocytes. Proc Natl Acad Sci U S A 1999; 96: 7962-7967.
[35] Aaltonen P, Luimula P, Astrom E, Palmen T, Gronholm T, Palojoki E, Jaakkola I, Ahola H, Tikkanen I and Holthofer H. Changes in the expression of nephrin gene and protein in experimental diabetic nephropathy. Lab Invest 2001; 81: 1185-1190.
[36] Sung SH, Ziyadeh FN, Wang A, Pyagay PE, Kanwar YS and Chen S. Blockade of vascular endothelial growth factor signaling ameliorates diabetic albuminuria in mice. J Am Soc Nephrol 2006; 17: 3093-3104.
[37] Menne J, Meier M, Park JK, Boehne M, Kirsch T, Lindschau C, Ociepka R, Leitges M, Rinta-Valkama J, Holthofer H and Haller H. Nephrin loss in experimental diabetic nephropathy is prevented by deletion of protein kinase C alpha signaling in-vivo. Kidney Int 2006; 70: 1456-1462.
[38] Menne J, Shushakova N, Bartels J, Kiyan Y, Laudeley R, Haller H, Park JK and Meier M. Dual inhibition of classical protein kinase C-alpha and protein kinase C-beta isoforms protects against experimental murine diabetic nephropathy. Diabetes 2013; 62: 1167-1174.
[39] Lamouille S and Derynck R. Cell size and invasion in TGF-beta-induced epithelial to mesenchymal transition is regulated by activation of the mTOR pathway. J Cell Biol 2007; 178: 437-451.
[40] Godel M, Hartleben B, Herbach N, Liu S, Zschiedrich S, Lu S, Debreczeni-Mor A, Lindenmeyer MT, Rastaldi MP, Hartleben G, Wiech T, Fornoni A, Nelson RG, Kretzler M, Wanke R, Pavenstadt H, Kerjaschki D, Cohen CD, Hall MN, Ruegg MA, Inoki K, Walz G and Huber TB. Role of mTOR in podocyte function and diabetic nephropathy in humans and mice. J Clin Invest 2011; 121: 2197-2209.
[41] Lloberas N, Cruzado JM, Franquesa M, Herrero-Fresneda I, Torras J, Alperovich G, Rama I, Vidal A and Grinyo JM. Mammalian target of rapamycin pathway blockade slows progression of diabetic kidney disease in rats. J Am Soc Nephrol 2006; 17: 1395-1404.
[42] Vollenbroker B, George B, Wolfgart M, Saleem MA, Pavenstadt H and Weide T. mTOR regulates expression of slit diaphragm proteins and cytoskeleton structure in podocytes. Am J Physiol Renal Physiol 2009; 296: F418-426.
[43] Chang X, Zhen X, Liu J, Ren X, Hu Z, Zhou Z, Zhu F, Ding K and Nie J. The antihelmenthic phosphate niclosamide impedes renal fibrosis by inhibiting homeodomain-interacting protein kinase 2 expression. Kidney Int 2017; 92: 612-624.